On the Validity of Analytic Potential Approximations for Galaxy Disks

[redacted]

Department of Astronomy & Steward Observatory, University of Arizona
ASTR513: Statistics & Computation, Fall 2022, Term Paper

[redacted]

The Miyamoto-Nagai (1975) profile has been the most popular analytic potential-density approximation in dynamical studies of exponential galaxy disks. In this work, I attempt to quantitatively investigate the validity of this approximation. I use existing simulation data of the equilibrium disk of the Large Magellanic Cloud which was initialized with an exponential profile. I fit the Miyamoto-Nagai function to the density profile data of this simulated disk using parallel Markov-Chain-Monte-Carlo. I find that the Miyamoto-Nagai profile is a significantly worse fit ($\chi^2_{\rm red,dof} = 13$) compared to the exponential profile, particularly for the vertical structure of the disk. Moreover, the Miyamoto-Nagai profile underestimates the total stellar mass of the disk by a factor of ~ 2, which leads to underestimates of accelerations and orbital velocities by a factor of 2 and 1.5 respectively in the disk outskirts. Thus, the Miyamoto-Nagai profile should be used with caution in studies involving dynamics of the outer disk.

1 Introduction

The potential field and the density distribution of a galaxy disk are the most important aspects in the study of galaxy dynamics, since the motion of stars and gas is almost completely determined by these two quantities. The potential and the density cannot be independently specified, since they are related by the Poisson equation:

$$\nabla^2\Phi = 4\pi G\rho, \tag{1}$$

where Φ is the potential and ρ is the density. A pair of real valued differentiable functions (Φ, ρ) which simultaneously satisfies eq. 1 and the boundary conditions associated with the disk is called a Potential-Density pair (PD pair in short).

Those PD pairs which can be expressed in terms of elementary functions are called analytic PD pairs. Such PD pairs have several advantages:

- They allow intuitive understanding of internal orbits of stars and effects of resonances (eg. [5]).
- They are used in tracer particle simulations which require precision control (eg. [3]).
- They are used to understand the dynamics of satellite galaxies (eg. [11]).
- Taylor expansion of PD pairs allow the understanding of harmonic and an-harmonic behaviour in the phase space (eg. [1]).
- The above allows detailed understanding of non-equilibrium behaviour of a galaxy disk in the presence of perturbations (eg. [1, 8]).

Observations of the brightness profile of galaxy disks suggests that its density profile has the following functional form:

$$\rho(r,z) = \frac{M}{4\pi a^2 b} sech^2\left(\frac{z}{b}\right) e^{-\left(\frac{r}{a}\right)}, \tag{2}$$

where M is a normalization mass, a is the radial scale length and b is the vertical scale length. The profile corresponding to eq. 2 is commonly known as the exponential profile. However, the potential corresponding to the exponential density profile is not analytic. Therefore, analytic approximations need to be employed which closely represent the exponential disk.

Several analytic prescriptions for potentials of galaxy disks exist - like the razor-thin potential [4], logarithmic potential [3] and the Miyamoto-Nagai potential [10]. Of these, the former two suffer from divergences either in themselves or their corresponding densities. However, the Miyamoto-Nagai potential does not have any such limitations, and has been the most popular choice (eg. [4, 1, 8, 11]).

The Miyamoto-Nagai potential has the following form:

$$\Phi(r,z) = \frac{GM}{\sqrt{r^2 + \left[a + \sqrt{z^2+b^2}\right]^2}}, \tag{3}$$

and the corresponding density is:

$$\rho(r,z) = \frac{b^2 M}{4\pi}\left[\frac{ar^2 + \left(a + 3\sqrt{z^2+b^2}\right)\left(a+\sqrt{z^2+b^2}\right)^2}{\left[r^2 + \left(a+\sqrt{z^2+b^2}\right)^2\right]^{\frac{5}{2}}\left(z^2+b^2\right)^{\frac{3}{2}}}\right] \tag{4}$$

Despite the widespread use of the Miyamoto-Nagai formulation, its validity as an approximation has not been investigated quantitatively in depth. In this work,

I attempt to perform a rigorous investigation of the same. In particular, I will try to address the following concerns:

- How well does the Miyamoto - Nagai profile represent the exponential disk ?
- Can the same parameters describing the exponential profile be used for the Miyamoto - Nagai approximation ?
- In which regimes does the Miyamoto - Nagai approximation break down ?
- What can be the physical consequences if the Miyamoto-Nagai approximation is not valid in certain regimes ?

I utilize the existing simulation data of Besla et al. 2012 [2] (hereafter B12) of the equilibrium disk of the Large Magellanic Cloud (LMC) for the above tests. In section 2, I describe the simulation data in more detail. In section 3, I shall develop the statistical framework to compare the Miyamoto-Nagai profile and the exponential profile. In section 4, I present the main results of the statistical analysis. I shall discuss the potential physical consequences of the results in section 5 and will finally summarize this work in 6.

2 Data Description

In what follows, I will interchangeably use cartesian and cylindrical coordinates. These coordinates are defined in Fig. 1. Origin of the coordinate system coincides with the center of mass of the galaxy disk.

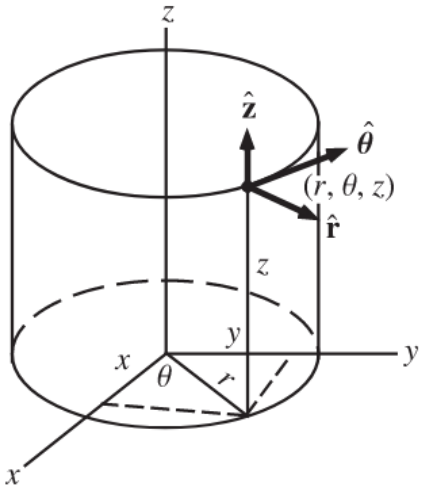

Figure 1: Cartesian and cylindrical coordinate system for the galaxy disk. Origin coincides with the center of mass of the disk. Source: Wolfram

I extract the position space information of stars (x, y, z) from the isolated LMC disk of B12 simulations. These simulations contain 10^6 star particles ($M_* = 2500\ M_\odot$ per particle) sampled in an exponential disk, and 10^5 Cold Dark Matter (CDM) particles ($M_{DM} = 1.8 \times 10^6\ M_\odot$ per particle) sampled in a Hernquist halo of scale radius 21.4 kpc. The radial scale length of the disk is set to 1.7 kpc, and the vertical scale length is set to 0.3 kpc. The projections of the density map of this disk are shown in Fig. 2.

3 Fitting Methodology

In this section, I develop the statistical framework for fitting the exponential and Miyamoto-Nagai density profile to the LMC disk of B12 simulations, with the main motivation of comparing the two fits. Since the simulated disk was realized with an exponential density profile in the first place, the parameters obtained through the fitting prescription for the exponential profile are expected to be consistent with the values mentioned in section 2. This would also serve to be a consistency check for the statistical framework itself.

First, I describe the procedure to obtain the radial and vertical density data of the simulated disk.

3.1 Obtaining Radial & Vertical Densities

I extract stars in a cuboidal volume defined by $x \in (-4.5, 4.5)$ kpc, $y \in (-0.5, 0.5)$ kpc, $z \in (-1, 1)$ kpc, and binned them in bins of $\delta x = 0.5$ kpc and $\delta z = 0.1$ kpc. I kept a single bin in the y direction. With this binning choice, the x direction corresponds to the r coordinate in the cylindrical system (Fig. 1). The $x - y$ and $x - z$ projections of this cuboidal volume are shown in Fig. 3.

I compute the density in each bin as follows:

$$\rho(x, z) = \frac{N(x, z) M_*}{\Delta V}, \tag{5}$$

where N represents the counts in each bin and ΔV represents the volume of that bin. I compute the error in each bin assuming the counts of star particles follow Poisson statistics:

$$\delta\rho(x, z) = \frac{\sqrt{N(x, z)} M_*}{\Delta V} \tag{6}$$

Having prepared the data for the density profile of the disk, next I present a sampling setup for fitting models to this data.

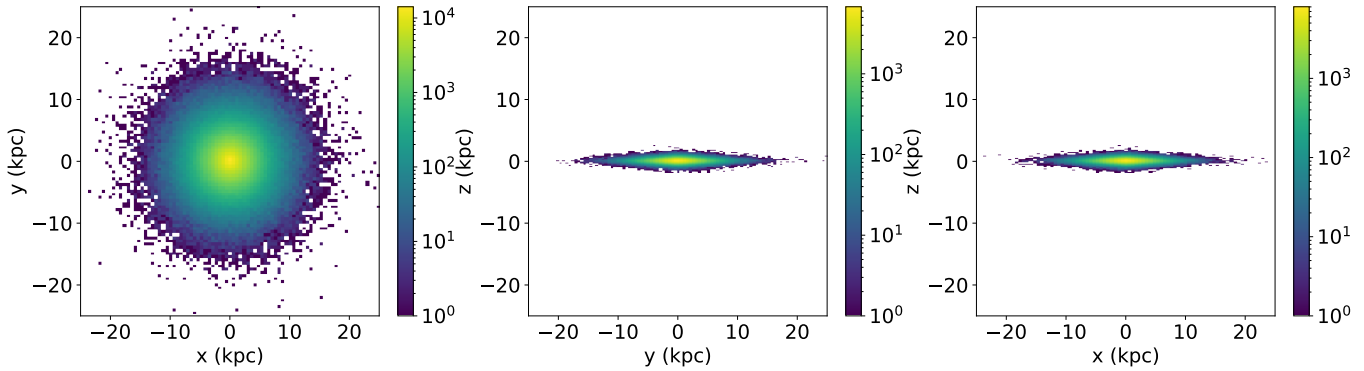

Figure 2: Stellar density map of the equilibrium LMC disk in B12 simulations [2]. Colorbar represents the counts of star particles.

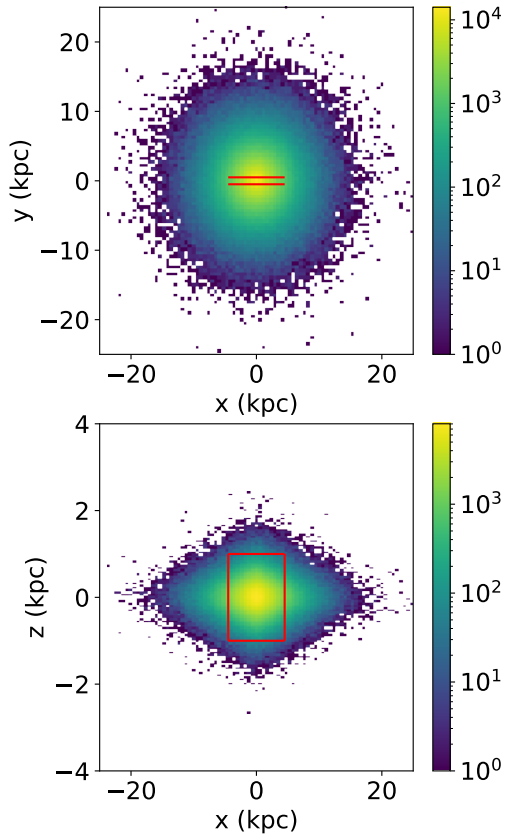

Figure 3: Cuboidal volume selected to compute the radial and vertical density profile data of the simulated disk of B12 [2]. Colorbar represents the counts of star particles.

3.2 Sampling Setup

I use the python based parallel MCMC sampler emcee [6] to sample the posterior distribution of the model parameters. I define the χ^2 as follows:

$$\chi^2 = \sum_{ij} \left(\frac{\rho_{\rm data}(r_i, z_j) - \rho_{\rm model}(r_i, z_j, a, b, M)}{\sigma_{ij}} \right)^2, \quad (7)$$

where model $\in$ {exponential profile, Miyamoto-Nagai profile}, and $\{i, j\}$ span over the density bins. I define the likelihood as follows:

$$\mathcal{L} = e^{-\frac{\chi^2}{2}} \quad (8)$$

I sample the parameters $a, b, log(M/M_\odot)$ using uniform priors, for both exponential and Miyamoto-Nagai models.

In eq. 7, I assumed the covariance matrix to be diagonal. I justify this assumption as follows. Consider two density bins $B_1 = (r_1, z_1)$ and $B_2 = (r_2, z_2)$, and let the corresponding densities be ρ_1 and ρ_2. Since the B12 simulations distribute the star particles in the disk by sampling them from the exponential density profile, ρ_1 and ρ_2 can be treated as random variables with means $\bar{\rho_1}$ and $\bar{\rho_2}$ respectively. The covariance between the two bins is:

$$\mathrm{Cov(B_1, B_2)} = \mathrm{E}[(\rho_1 - \bar{\rho_1})(\rho_2 - \bar{\rho_2})]$$

which evaluates to:

$$\mathrm{Cov(B_1, B_2)} = \mathrm{E}[\rho_1 \rho_2] - \bar{\rho_1}\bar{\rho_2}$$

Now, $E[\rho_1\rho_2] \approx E[\rho_1]E[\rho_2] = \bar{\rho_1}\bar{\rho_2}$ since the sampling of the two bins B_1 and B_2 can be treated as independent processes. This is so because the distance between any two bins in our data is much greater than the gravitational softening length adopted in the B12 simulations. Thus, $\mathrm{Cov(B_1, B_2)} \approx 0$, hence the covariance matrix can be taken to be diagonal.

3.3 Fitting of Exponential and Miyamoto-Nagai Density Profiles

I fit the exponential density profile and the Miyamoto-Nagai density profile to the simulated density data by

adopting the following priors for the model parameters:

- $a \in (0.1, 5)$ kpc
- $b \in (0.1, 0.5)$ kpc
- $log(M/M_\odot) \in (9, 10)$

The above priors are physically motivated, and correspond to the rough range of values suggested by observations of the LMC disk. I ran the sampler on 200 parallel chains with a chain length of 200, parallelizing on 8 CPUs. The chains have nicely converged, as illustrated in Fig. 4.

4 Results

Fig. 5 shows the triangle plot of posterior contours of the parameters of both the exponential and the Miyamoto-Nagai models. The triangle plots and the subsequent analysis of the fits have been performed with the getdist python package [9].

The marginalized posteriors of the fit parameters resemble a Gaussian distribution. There seems to be a correlation between the multiplier mass $\log\left(\frac{M}{M_\odot}\right)$ and the radial scale length a in both the models. However, given the range of values along the mass axis, this correlation is insignificant.

Next, I present the fits for the exponential and Miyamoto-Nagai models in Fig. 6 and Fig. 7 respectively. For computing the radial density profile, I consider all radial bins at $z = 0.05$ kpc. For computing the vertical density profile, I consider all vertical bins at $r = 0.25$ kpc. The bottom panels of Figures 6 and 7 show the residuals. The residuals are computed as follows:

$$\text{Residual} = \rho_{\text{fit}}(\text{r}, \text{z}) - \rho_{\text{data}}(\text{r}, \text{z}), \tag{9}$$

where ρ_{fit} corresponds to the best fit. The errors on the residuals are computed as follows:

$$\delta_{\text{Residual}} = \sqrt{\delta\rho_{\text{fit}}^2 + \delta\rho_{\text{data}}^2}, \tag{10}$$

where $\delta\rho_{\text{data}}$ is the Poisson error on density data as described in section 2, and $\delta\rho_{\text{fit}}$ is the error on the best fit density model. The latter error is computed by treating density as a derived parameter on the MCMC parameter chains, and then computing its one standard deviation.

The exponential profile fits very well to the density profile data. This is to be expected since the B12 disk was initialized with an exponential profile in the first place. The vertical density profile tapers off at low values of z, reflecting the $sech^2$ nature of eq. 2.

The Miyamoto-Nagai profile fits the radial density profile data reasonably well, however it overestimates the density around $r = 1.5$ kpc, as is evident from the residuals. As for the vertical direction, the model seems to underestimate the density for low values of z and overestimates the same at high values of z. This is again evident from the residuals.

5 Discussion

We realized in section 4 that the Miyamoto-Nagai profile may not be a good fit to the exponential profile in certain regimes. In this section, we shall try to quantify the above in more detail, as well as discuss its potential consequences.

5.1 Quantitative Comparison of the Fits

Corresponding to the exponential profile, I obtain the following best fit parameters (along with one standard deviation errors):

- $a = 1.78 \pm 0.01$ kpc
- $b = 0.343 \pm 0.001$ kpc
- $log(\frac{M}{M_\odot}) = 9.405 \pm 0.004$

Whereas, corresponding to the Miyamoto-Nagai profile, I obtain:

- $a = 2.14 \pm 0.01$ kpc
- $b = 0.326 \pm 0.001$ kpc
- $log(\frac{M}{M_\odot}) = 9.514 \pm 0.003$

Thus, there is a strong tension between the parameters of the exponential profile and Miyamoto-Nagai profile. This is also evident from the posteriors in Fig. 8.

I also compute the reduced χ^2 per degree-of-freedom

$$\chi^2_{red,dof} = \frac{\chi^2_{red}}{N_{dof}}$$

for the two fits in order to quantify the goodness-of-fit. Here, N_{dof} denotes the number of degrees-of-freedom. They are computed as follows:

$$N_{dof} = N_{data} - N_{params},$$

where N_{data} is the number of data points and N_{params} is the number of parameters. For our purpose, N_{data} is the number of density bins = 360 and $N_{params} = 3$ (since the potential models are described by 3 parameters). Thus, $N_{dof} = 357$.

For the exponential profile, I obtain $\chi^2_{red,dof} = 1.03$. This signifies a very good fit, which is expected since the simulated LMC disk is initialized with an exponential profile. However, for the Miyamoto-Nagai profile, $\chi^2_{red,dof} = 13.42$, which signifies a much worse fit.

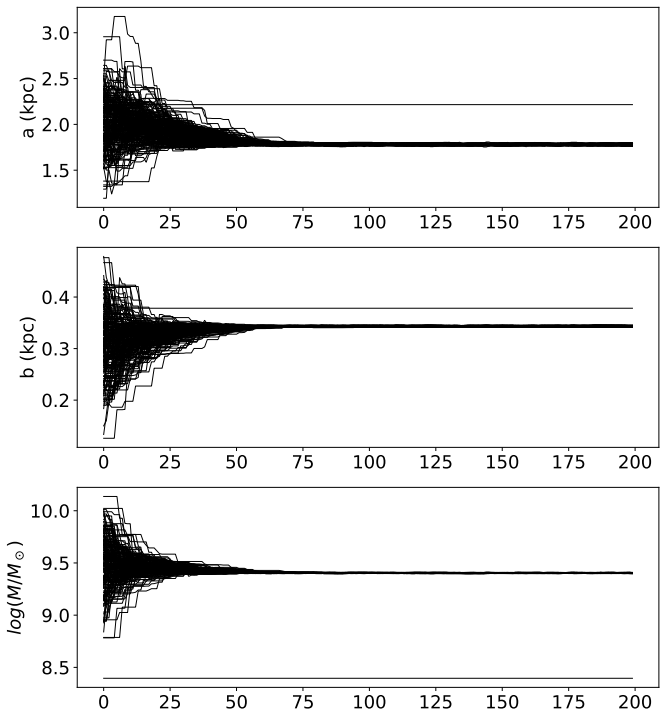

(a) MCMC chains for the exponential profile fit.

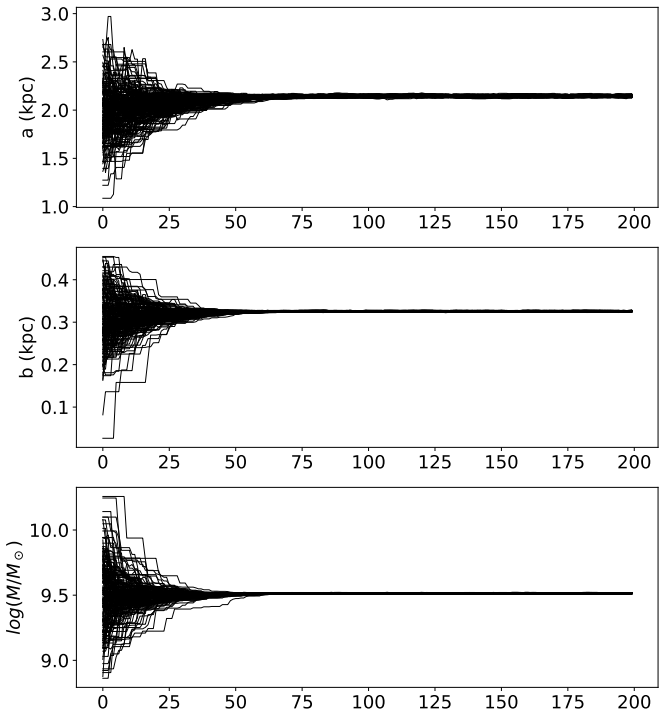

(b) MCMC chains for the Miyamoto-Nagai profile fit

Figure 4: MCMC chains for the exponential and Miyamoto-Nagai fits. x-axis shows the chain length. The chains have nicely converged.

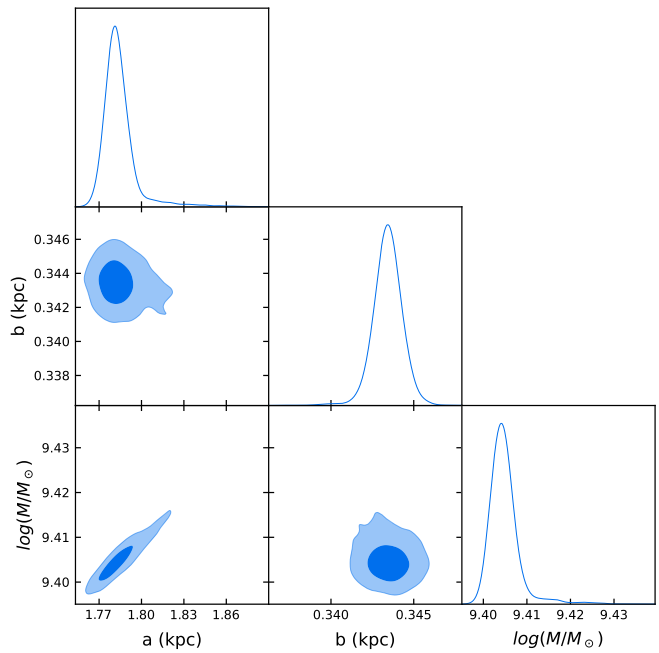

(a) Triangle plot for the exponential profile fit to the density data.

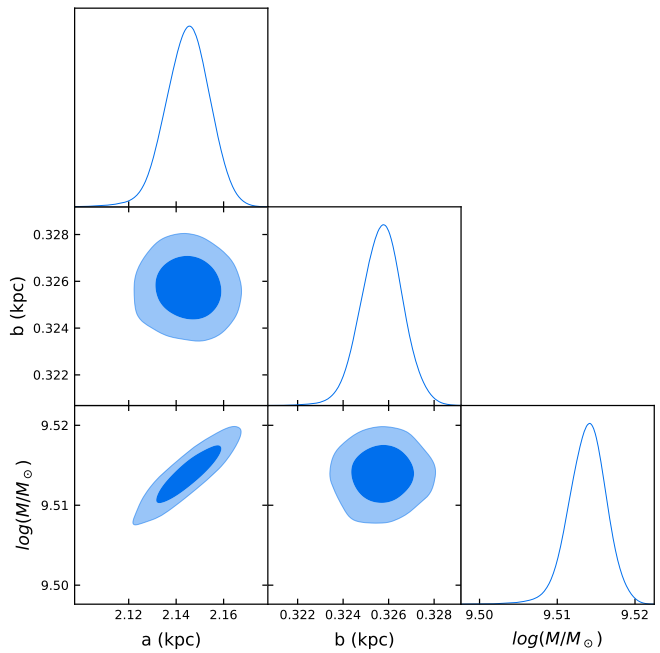

(b) Triangle plot for the Miyamoto-Nagai profile fit to the density data.

Figure 5: Triangle plots showing contours and marginalized posteriors for the exponential and Miyamoto-Nagai profile fits. Best fit parameters of the expoential fit are consistent with what was initialized in the B12 [2] simulations.

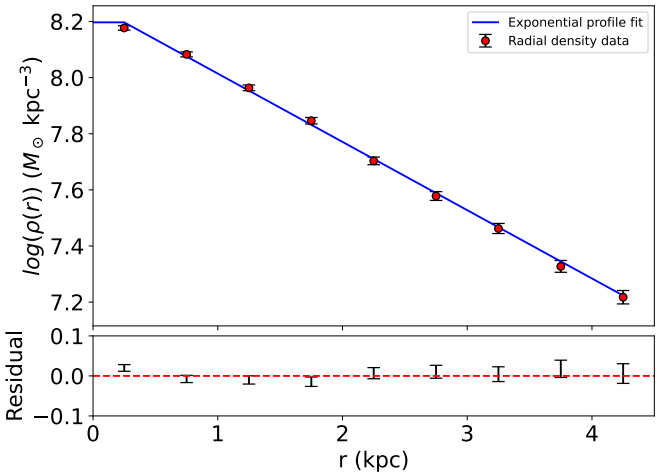

(a) Exponential profile best fit to the radial density data.

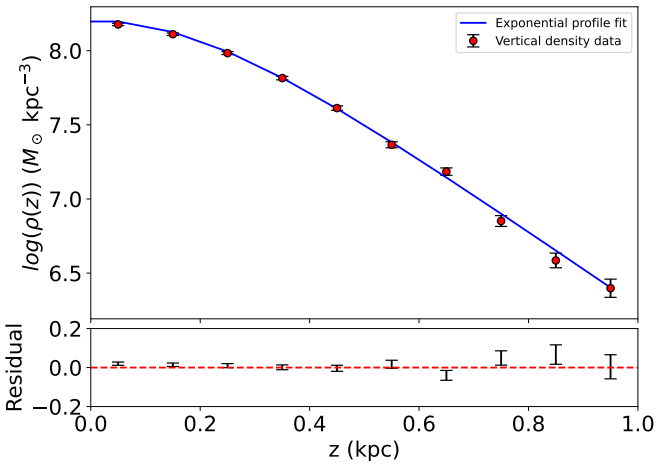

(b) Exponential profile best fit to the vertical density data.

Figure 6: Best fit model of the exponential profile with residuals.

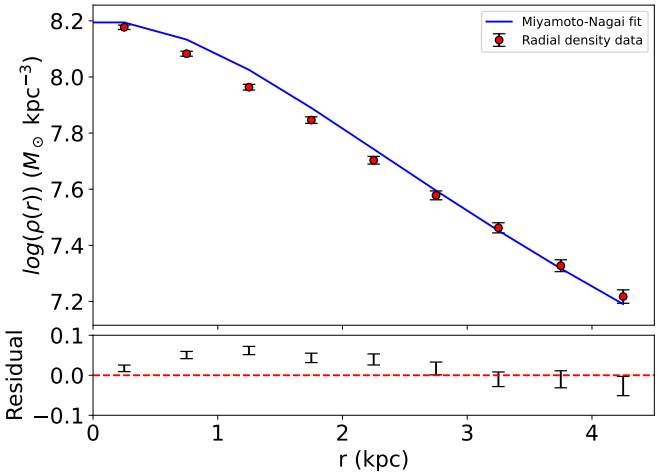

(a) Miyamoto-Nagai profile best fit to the radial density data.

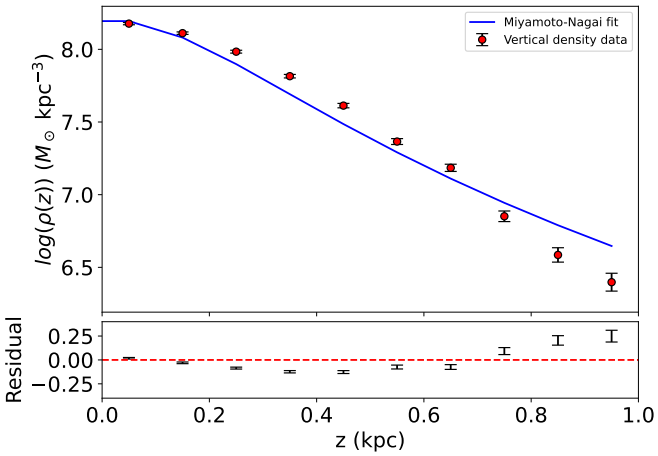

(b) Miyamoto-Nagai profile best fit to the vertical density data.

Figure 7: Best fit model of the Miyamoto-Nagai profile with residuals.

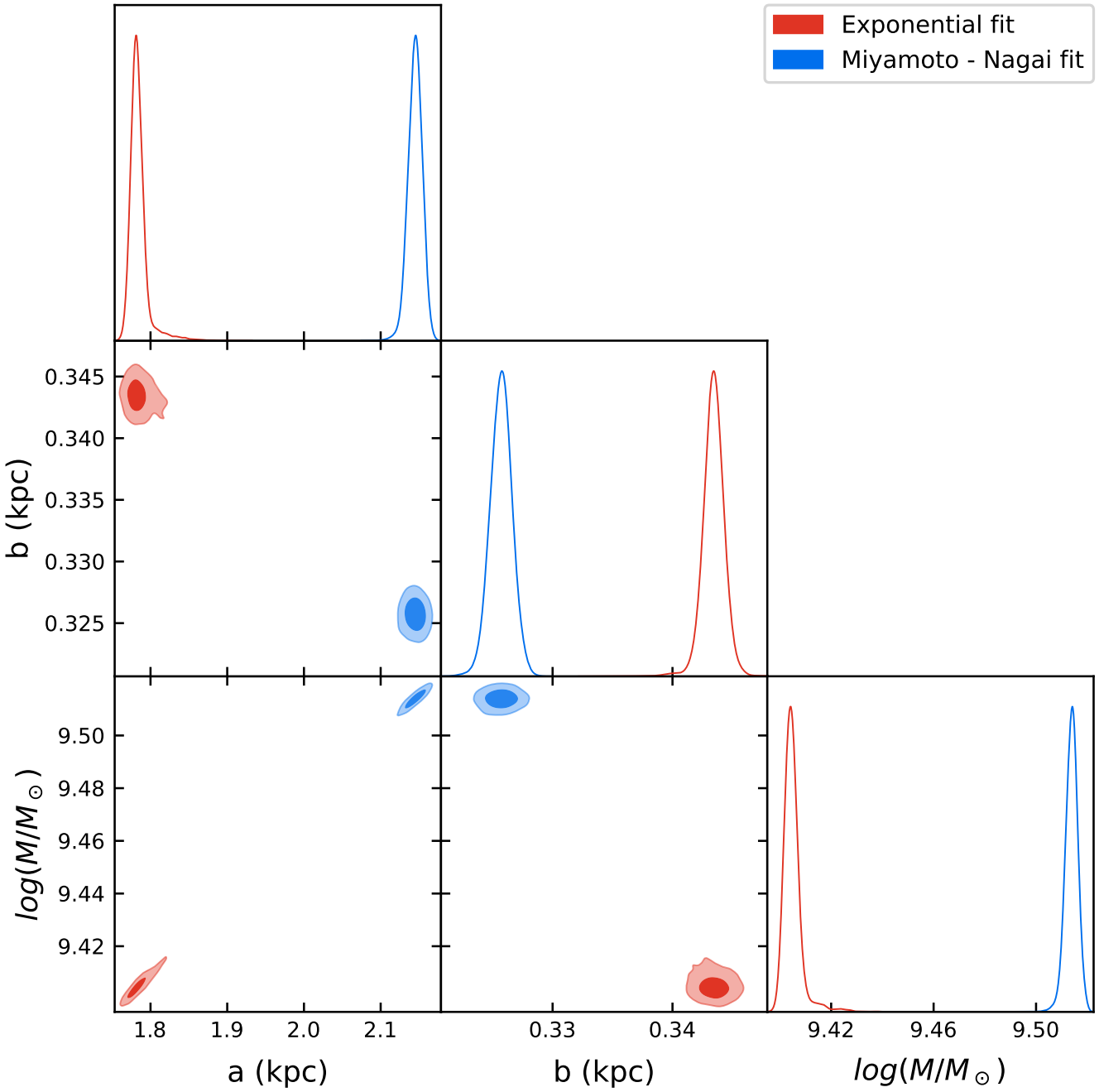

Figure 8: Posteriors of the parameters of the exponential profile and the Miyamoto-Nagai profile. There is a strong tension between the parameter values of the two profiles.

In observational studies, the mass-to-light ratio of the galaxy disk is used to convert the observed brightness profile to the density profile. This conversion also has errors associated with it, which I have not taken into account. I expect that taking these errors into account will lower the $\chi^2_{red,dof}$ corresponding to the Miyamoto-Nagai profile, and will return a slightly better fit. However, the latter will still be a poor fit when compared to the exponential profile.

5.2 Mass Profile Comparison

I shall compare the mass profile of the disk as obtained from the exponential and Miyamoto-Nagai profiles in order to motivate a physical consequence of the breakdown of the Miyamoto-Nagai approximation.

The mass profile is defined as the stellar mass of the disk contained inside a radius r (in cylindrical coordinates), as a function of r. It is computed as follows:

$$M(r) = 2\pi \int_0^r \int_{z=-2\text{ kpc}}^{2\text{ kpc}} \rho(r,z) r^2 dr dz, \qquad (11)$$

where I have chosen the $z-$ limits such that almost the entire vertical distribution of stats is encapsulated in the integral. At large r, the mass profile tends to the total mass of the disk.

I compute the mass profile of the disk between $r = 0.5$ kpc and $r = 20$ kpc in bins of 0.5 kpc. I use the scipy pacakge *dblquad* for the numerical integration of eq. 11. The mass profile for the disk and the corresponding Miyamoto-Nagai fit are shown in Fig. 9.

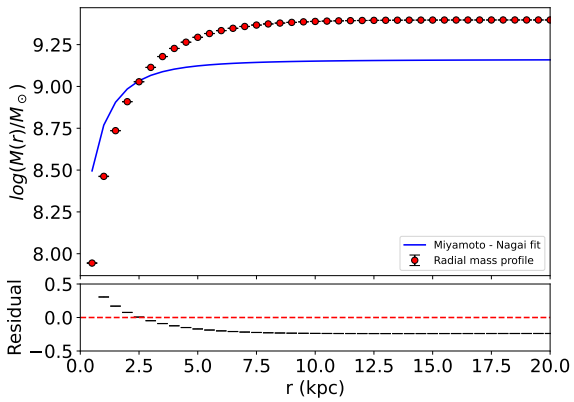

Figure 9: The radial mass profile of the simulated disk (red data points with error bars) as well as the Miyamoto-Nagai fit (blue line). Fit residuals are shown in the bottom panel.

The Miyamoto-Nagai profile ends up underestimating the total mass (M_T) of the disk by almost a factor of 2. This has several consequences when it comes to modelling dynamical processes in the outskirts of a galaxy disk.

Near the outskirts, the gravitational force due to a disk is proportional to the mass of the disk. Thus, an underestimate of the mass by a factor of 2 will lead to underestimate of the forces (hence accelerations) in the outskirts by a factor of 2. This will directly affect the orbits of satellite galaxies and globular clusters.

Moreover, near the outskirts the angular velocity of circular orbits $\Omega \propto \sqrt{M_T}$. Thus, Miyamoto-Nagai profile will lead to an underestimate of the same by a factor of ~ 1.5. This will directly affect the dark matter distribution of the galaxy, as well as how stellar orbits in the disk outskirts respond to perturbations.

5.3 Future Scope

From the above discussion it is clear that the Miyamoto-Nagai potential is not a good approximation to a galaxy disk near the outskirts. Thus, alternative analytic potential approximations must be considered in order to best represent a galaxy disk.

One such choice can be the combination of multiple Miyamoto-Nagai potentials, patched together such that the resulting profile is differentiable everywhere (eg. [12]).

From Fig. 7b, it is evident that the Miyamoto-Nagai profile underestimates the density at low values of z and overestimates the same at high values. Thus, combining the Miyamoto-Nagai profile with a potential function that has a large value at low values of z and decreases rapidly as z rises can *correct* the Miyamoto-Nagai profile. Once such function is the analytical potential that is used to describe galaxy bulges, i.e., the Hernquist potential [7]. Thus, combining the Miyamoto-Nagai potential with a Hernquist potential can also be an alternative analytical potential formulation which mitigates the issues of the former.

A key point to note here is that the LMC has an unusually thicker disk. Thus, the limitations of the Miyamoto-Nagai approximations are amplified for such a disk. For a disk like the Milky-Way, which is relatively thin, the Miyamoto-Nagai approximation is expected to have a better fit.

6 Conclusion

The Miyamoto-Nagai potential-density pair [10] is the most popular analytic approximation for thick exponential galaxy disks. In this work, I explored quantitatively the validity of this approximation, and asked the following questions in particular:

- How well does the Miyamoto - Nagai profile represent the exponential disk, and can the same pa-

rameters describing the exponential profile be used for the Miyamoto-Nagai approximation ?

- In which regimes does the Miyamoto - Nagai approximation break down, and what can be the physical consequences thereof ?

In order to perform this study, I utilized existing simulation data of Besla et al. 2012 [2] of the equilibrium disk of the Large Magellanic Cloud (LMC). This simulated LMC disk had been initialized with an exponential profile in [2].

I obtained the density map of the simulated LMC disk by constructing a cuboidal volume centered at the center of the disk, and binned the same in x, y and z directions. I obtained errors on the density map by assuming star particle counts follow Poisson statistics.

I used parallel Markov-Chain-Monte-Carlo based χ^2 minimization to fit both Miyamoto-Nagai profile and exponential profile to the density map of the simulated LMC disk. I adopted uniform priors for radial, vertical scale lengths and normalization mass of the profiles.

The main results are summarized as follows:

- Miyamoto-Nagai fit yields a much worse reduced χ^2 per degree of freedom ($\chi^2_{red,dof} \approx 13$) compared to the exponential fit ($\chi^2_{red,dof} \approx 1$).
- The Miyamoto-Nagai approximation is not a good representation of the vertical density profile of the disk. It underestimates the density near the disk mid-plane and overestimates the density at large distances from the mid-plane.
- The parameters of the Miyamoto-Nagai fit are in strong tension with those of the exponential fit, thus same parameter values cannot be used for both profiles.

Moreover, the Miyamoto-Nagai profile underestimates the total disk mass by a factor of 2. Thus, it will underestimate the accelerations and orbital speeds near the disk outskirts by a factor of 2 and 1.5 respectively. This will have important consequences for the dynamical modeling of stellar and satellite orbits near galaxy outskirts.

In conclusion, the Miyamoto-Nagai profile has several limitations, as has been pointed out in this work. Thus, alternative analytical potential formulations should be used in dynamical studies focusing on outer regions of a galaxy disk.

I thank Dr. Gurtina Besla for making the Besla et al. 2012 [2] simulation data available for this work, as well as for helpful discussions on galaxy potentials. I thank Dr. Tim Eifler for providing me the opportunity to work on this term project through the ASTR 513: Statistical & Computational Methods course. This work made use of python packages like Numpy, Scipy, Astropy and Matplotlib. The code repository of this work can be found on `https://github.com/himanshrathore/astr513project`, and queries can be addressed to the corresponding author through the email provided.

References

[1] T. Antoja et al. "A dynamically young and perturbed Milky Way disk". In: *Nature* 561.7723 (Sept. 2018), pp. 360–362. DOI: 10.1038/s41586-018-0510-7. arXiv: 1804.10196 [astro-ph.GA].

[2] Gurtina Besla et al. "The role of dwarf galaxy interactions in shaping the Magellanic System and implications for Magellanic Irregulars". In: *Mon. Not. Roy. Astron. Soc.* 421.3 (Apr. 2012), pp. 2109–2138. DOI: 10.1111/j.1365-2966.2012.20466.x. arXiv: 1201.1299 [astro-ph.GA].

[3] Jo Bovy. "galpy: A python Library for Galactic Dynamics". In: *Astrophysical Journal Supplement* 216.2, 29 (Feb. 2015), p. 29. DOI: 10.1088/0067-0049/216/2/29. arXiv: 1412.3451 [astro-ph.GA].

[4] G. N. Candlish et al. "Phase mixing due to the Galactic potential: steps in the position and velocity distributions of popped star clusters". In: *Mon. Not. Roy. Astron. Soc.* 437.4 (Feb. 2014), pp. 3702–3717. DOI: 10.1093/mnras/stt2166. arXiv: 1311.1507 [astro-ph.GA].

[5] Kathryne J. Daniel et al. "When Cold Radial Migration is Hot: Constraints from Resonant Overlap". In: *Astrophysical Journal* 882.2, 111 (Sept. 2019), p. 111. DOI: 10.3847/1538-4357/ab341a. arXiv: 1907.10100 [astro-ph.GA].

[6] Daniel Foreman-Mackey et al. "emcee: The MCMC Hammer". In: *Pub. Astron. Soc. Pacific* 125.925 (Mar. 2013), p. 306. DOI: 10.1086/670067. arXiv: 1202.3665 [astro-ph.IM].

[7] Lars Hernquist. "An Analytical Model for Spherical Galaxies and Bulges". In: *Astrophysical Journal* 356 (June 1990), p. 359. DOI: 10.1086/168845.

[8] Chervin F. P. Laporte et al. "Footprints of the Sagittarius dwarf galaxy in the Gaia data set". In: *Mon. Not. Roy. Astron. Soc.* 485.3 (May 2019), pp. 3134–3152. DOI: 10.1093/mnras/stz583. arXiv: 1808.00451 [astro-ph.GA].

[9] Antony Lewis. "GetDist: a Python package for analysing Monte Carlo samples". In: *arXiv e-prints*, arXiv:1910.13970 (Oct. 2019), arXiv:1910.13970. arXiv: 1910 . 13970 [astro-ph.IM].

[10] M. Miyamoto and R. Nagai. "Three-dimensional models for the distribution of mass in galaxies." In: *Pub. Astron. Soc. Japan* 27 (Jan. 1975), pp. 533–543.

[11] Ekta Patel et al. "The Orbital Histories of Magellanic Satellites Using Gaia DR2 Proper Motions". In: *Astrophysical Journal* 893.2, 121 (Apr. 2020), p. 121. DOI: 10.3847/1538-4357/ab7b75. arXiv: 2001.01746 [astro-ph.GA].

[12] R. Smith et al. "Simple and accurate modelling of the gravitational potential produced by thick and thin exponential discs". In: *Mon. Not. Roy. Astron. Soc.* 448.3 (Apr. 2015), pp. 2934–2940. DOI: 10.1093/mnras/stv228. arXiv: 1502.00627 [astro-ph.GA].